



1 **Estimation of pollen counts from light scattering intensity when sampling multiple pollen taxa —**
2 **Establishment of Automated Multi-taxa Pollen Counting Estimation System (AME System)—**

3 Kenji Miki^{1*}, Shigeto Kawashima¹

4

5 ¹ Graduate School of Agriculture, Kyoto University, Oiwake-cho, Kitashirakawa, Sakyo-ku, Kyoto 606-8502,
6 Japan

7

8 *Correspondence to: Kenji Miki (kmiki@elsi.jp)

9

10 **Abstract.**

11 Laser optics have long been used in pollen counting systems. To clarify the limitations and potential new
12 applications of laser optics for automatic pollen counting and discrimination, we determined the light scattering
13 patterns of various pollen types, tracked temporal changes in these distributions, and introduced a new theory for
14 automatic pollen discrimination. Our experimental results indicate that different pollen types often have different
15 light scattering characteristics, as previous research has suggested. Our results also show that light scattering
16 distributions did not undergo significant temporal changes. Further, we show that the concentration of two
17 different types of pollen could be estimated separately from the total number of pollen grains by fitting the light
18 scattering data to a probability density curve. These findings should help realize a fast and simple automatic pollen
19 monitoring system.

20

21



22 1 Introduction

23 Pollen counting is a time-consuming and labor-intensive task that requires professional skills. However, recent
24 technological developments have made automatic pollen sampling and identification possible (Buters et al. 2018),
25 for example, with recognition systems using microscopic images of pollen grains (Boucher et al. 2002; Ranzato
26 et al. 2007; Oteros et al. 2015), pollen color patterns from pollen images (Landsmeer et al. 2009), fluorescence
27 emission signals, (Swanson and Huffman 2018; Mitsumoto et al. 2009; Mitsumoto et al. 2010; Richardson et al.
28 2019), light scattering (Crouzy et al. 2016; Šaulienė et al. 2019, holographic images (Sauvageat et al. 2019), size
29 and morphological characteristics (O'Connor et al. 2013), real-time PCR (Longhi et al. 2009), texture and infrared
30 patterns of microscopic images of pollen (Marcos et al. 2015; Gottardini et al. 2007; Chen et al. 2006), or a
31 combination of several of these. Many studies applied machine learning algorithms to the problem (Punyasena et
32 al. 2012; Tcheng et al. 2016; Crouzy et al. 2016; Gonçalves et al. 2016; Gallardo-Caballero et al. 2019; Šaulienė
33 et al. 2019). These automated pollen identification methods have been applied not only to aerobiological research
34 but also to palynological studies for the identification of fossilized pollen (France et al. 2000; Kaya et al. 2014; Li
35 et al. 2004; Zhang et al. 2004; Rodríguez-Daminán et al. 2006).

36 Analysis using light scattering patterns has a particular focus, with several methods being developed for
37 establishing an automatic aerosol or bioaerosol counting system (Huffman et al. 2016). For example, polarization
38 signals can be used to discriminate *Cryptomeria japonica* from polystyrene spherical particles (Iwai 2013).
39 Studies applying machine learning algorithms have shown that light scattering patterns can be used for automatic
40 classification and counting of multiple pollen taxa simultaneously (Crouzy et al., 2016; Sauliene et al., 2019).
41 Other studies have applied statistical techniques to compare the light scattering data and number of multiple taxa
42 pollen grains (Kawashima et al. 2007, 2017; Matsuda and Kawashima 2018). Surbek et al. (2011) also studied the
43 discrimination method for Hazel, Birch, Willow, Ragweed, and Pine pollen showing that they have distinct
44 characteristics in the backward and sideward light scattering patterns.

45 In the present study, light scattering patterns from various pollen taxa are investigated with a KH-3000 to verify
46 whether they have different light scattering patterns. A novel method is also proposed to discriminate between
47 two taxa with similar scattering patterns.

48

49 2 Materials and methods

50 A protection cylinder (radius = 5 cm, height = 30 cm) was attached to the sampling tube of a KH-3000-01 laser-
51 optics-based automatic pollen counter (Yamatronics, Japan). The KH-3000-01 is a widely used automatic pollen
52 counting system (e.g. Wang et al. 2014; Takahashi et al. 2001; Miki et al. 2017, 2019; Kawashima et al. 2007,
53 2017; Matsuda and Kawashima 2018). A laser irradiates particles that pass through the sampling system and the
54 forward and side scattering signals from each particle are recorded. In this study pollen grains from known taxa
55 were injected through an injection tube in the wall of the protection cylinder and sampled in the KH-3000-01. The
56 side and front scattering intensities were evaluated by converting the light intensity into a voltage.

57 2.1 Temporal changes in light scattering patterns

58 *Alnus* pollen grains were directly sampled from catkins on a tree growing at the Swiss Federal Office of
59 Meteorology and Climatology on a sunny morning on February 28 2019. Light scattering measurements were
60 taken using the fresh pollen grains soon after they were collected. The remaining pollen grains were stored in
61 tubes and scattering patterns were reevaluated after storing them for 1 h, 2 h, 6 h, and 10 days. Multiple
62 comparisons using the Bonferroni method were performed on the side and front scattering data to assess whether
63 the light scattering distributions showed changes after storage. Bonferroni method is a multiple comparison
64 method used for non-parametric data sets. In order to carry out the multiple comparison, 316 scattering data of
65 each taxa were picked up because the Bonferroni method requires the same amount of data of each taxa and 316
66 scattering data was the smallest amount of data amongst each time step (10 day).

67 2.2 Light scattering patterns of different pollen taxa

68 Dried pollen grains from *Alnus*, *Ambrosia*, *Artemisia*, *Betula*, *Castanea*, *Cedrus*, *Corylus*, *Fagus*, *Fraxinus*,
69 *Helianthus*, *Olea*, *Phleum*, *Quercus*, *Taxus*, and *Zea* were sampled in a similar way. These taxa are representative
70 of the pollen types commonly observed in Europe. After collecting the light scattering distributions of each pollen
71 type, multiple comparisons using the Bonferroni method were performed to evaluate whether these distributions
72 differ significantly from each other. In order to carry out the multiple comparison, 210 scattering data of each taxa
73 were picked up based on the smallest amount of data amongst the taxon (*Helianthus*).

74 2.3 Automatic discrimination theory



75 To carry out simple and fast automatic pollen discrimination, the number of pollen grains of each type from the
 76 total number of pollen grains was calculated as follows.

77 For two different types of pollen (A and B) in the side scattering intensity range $a - b$ and in the front scattering
 78 intensity range $c - d$, the following equation holds:

$$\begin{aligned} \int_a^b P_{A_{side}}(x) dx &= p_{A_{side}} \\ \int_a^b P_{B_{side}}(x) dx &= p_{B_{side}} \\ \int_c^d P_{A_{front}}(x) dx &= p_{A_{front}} \\ \int_c^d P_{B_{front}}(x) dx &= p_{B_{front}} \end{aligned} \quad (1)$$

79 where P is the representative probability density function of the scattering intensity. p is the representative
 80 probability of the scattering intensity of each pollen grain lying in the integration intervals.

81 Next, the scattering intensity distribution that gives the number of pollen grains at each scattering intensity was
 82 fitted to a distribution function. In this experiment, the normal distribution was fitted to the number of pollen
 83 grains in every 100 mV steps. The gaussian function is written as:

$$f(x) = \frac{\alpha}{\sqrt{2\pi}} \exp\left\{-\frac{(x - \mu)^2}{2\sigma^2}\right\} + c \quad (2)$$

84 where α and c are coefficients, μ is the mean, σ is the standard deviation.

85 Fitting the data to the normal distribution function enables one to calculate the probability of a pollen grain
 86 showing a certain light scattering intensity. The probability density of the normal distribution function (P) is
 87 written as:

$$P(x) = \frac{1}{\sqrt{2\pi\sigma^2}} \exp\left\{-\frac{(x - \mu)^2}{2\sigma^2}\right\} \quad (3)$$

88 Fitting was performed by nonlinear optimization. The normal distribution was chosen so that we can handle the
 89 light scattering plots using a known function.

90 Equation (1) gives

$$\begin{aligned} C_1 p_{A_{side}} N_A + C_2 p_{B_{side}} N_B &= n_{side \ a-b} \\ C_3 p_{A_{front}} N_A + C_4 p_{B_{front}} N_B &= n_{front \ c-d} \\ N_A + N_B &= N_{total} \end{aligned} \quad (5)$$

91 Here, N is the number of sampled pollen grains of each pollen type, which are the values to be calculated. N_{total}
 92 is the total number of sampled pollen grains and n is the total number of sampled pollen grains in the integration
 93 interval, which are known numbers. C is the correction factor defined by the following equation:

$$\begin{aligned} C &= \frac{\int_{-\infty}^{+\infty} P(x) dx}{\int_0^{4500} P(x) dx} \\ &= \frac{1}{\int_0^{4500} P(x) dx} \end{aligned} \quad (6)$$

94 C is needed for renormalization of the probability distribution because the device KH-3000-01 is able to detect
 95 the scattering intensity only in the range of 0–4500mV.

96 By solving two equations in Eq. (5), N_A and N_B will be theoretically estimated.



97 In this paper, *Alnus* and *Artemisia* were chosen as examples to evaluate the usability of the theory above. Because
98 fitting worked well in the range of 600–800mV for the side scattering and 300–500mV for the front scattering,
99 $a = 600$, $b = 800$, $c = 300$ and $d = 500$ were substituted in Eq. (5). The evaluation tests were carried out five
100 times using the light scattering data for both *Alnus* and *Artemisia* (Fig. 1).

101 The magnitude of the estimation error is calculated as follows.

$$\text{error (\%)} = \frac{|\text{actual} - \text{estimation}|}{\text{actual}} \times 100 \quad (7)$$

102

103

104 3 Results

105 3.1 Temporal changes in light scattering pattern

106 The scattering distribution of *Alnus* pollen (Fig. 2) showed no significant temporal changes in scattering
107 distributions in 10 day (Table 1).

108 3.2 Light scattering distributions of different pollen taxa

109 Pollen grains with smaller sizes tend to show smaller voltage values (Fig. 3).. The results of the multiple
110 comparisons (Table 2) indicated that there is always a significant different between side and front scattering
111 between two different pollen types except between:

112 Side scattering: *Alnus-Ambrosia*, *Alnus-Corylus*, *Alnus-Olea*, *Ambrosia-Fraxinus*, *Betula-Phleum*, *Betula-*
113 *Quercus*, *Corylus-Olea*, *Fagus-Zea*, *Artemisia-Fraxinus*, *Helianthus-Zea*, *Phleum-Quercus*

114 Front scattering: *Alnus-Corylus*, *Alnus-Quercus*, *Ambrosia-Artemisia*, *Ambrosia-Fraxinus*, *Artemisia-Fraxinus*,
115 *Betula-Phleum*, *Betula-Quercus*, *Castanea-Olea*, *Cedrus-Helianthus*, *Corylus-Quercus*, *Fagus-Helianthus*,
116 *Fagus-Zea*, *Phleum-Quercus*

117 3.3 Automatic counting

118 Counting the number of pollen grains of each type can be carried out by solving the two equations from Eq. (5),
119 side ($n_{\text{side } a-b}$) and front ($n_{\text{front } c-d}$), side ($n_{\text{side } a-b}$) and total (N_{total}), front ($n_{\text{front } c-d}$) and total (N_{total}). The
120 parameters of the probability density curve of the side and the front (Fig. 4) light scattering distributions of *Alnus*
121 and *Artemisia* were estimated as follows:

$$122 P_{\text{Alnus}_{\text{side}}}(\alpha, \mu, \sigma, c) = (433.58, 555.13, 223.85, 14.74)$$

$$123 P_{\text{Alnus}_{\text{front}}}(\alpha, \mu, \sigma, c) = (588.98, 419.45, 192.67, 10.31)$$

$$124 P_{\text{Alnus}_{\text{front}}}(\alpha, \mu, \sigma, c) = (600.25, 348.67, 159.96, 16.25)$$

$$125 P_{\text{Artemisia}_{\text{front}}}(\alpha, \mu, \sigma, c) = (1028.57, 202.64, 107.32, 13.00)$$

126 The results (Fig. 5) show that the estimated number of pollen grains had average errors of 46.80%, 33.9%, 39.12%
127 for *Alnus* and 30.81%, 18.77%, 20.57% for *Artemisia* (Table 3).

128

129 4 Discussion

130 Temporal changes in the shapes of pollen grains are expected to affect the changes in light scattering patterns.
131 However, our experimental data indicate that light scattering patterns show little to no changes over time (up to
132 at least 10 days). Thus, there should be no problem using pollen grains that are either fresh or have been stored
133 for several days for studies with the KH-3000. Further investigation is required to understand whether this is true
134 for species other than *Alnus* and for longer periods of time. Understanding the morphological stability of each
135 pollen type would be helpful to understand the temporal stability of light scattering patterns.

136 Light scattering data from various pollen taxa indicate that it is not possible to discriminate between the side
137 scattering patterns of *Alnus* vs *Ambrosia*, *Alnus* vs *Corylus*, *Alnus* vs *Olea*, *Ambrosia* vs *Fraxinus*, *Betula* vs



138 *Phleum*, *Betula* vs *Quercus*, *Corylus* vs *Olea*, *Fagus* vs *Zea*, *Artemisia* vs *Fraxinus*, *Helianthus* vs *Zea*, *Phleum*
139 vs *Quercus* and the front scattering patterns between *Alnus* vs *Corylus*, *Alnus* vs *Quercus*, *Ambrosia* vs *Artemisia*,
140 *Ambrosia* vs *Fraxinus*, *Artemisia* vs *Fraxinus*, *Betula* vs *Phleum*, *Betula* vs *Quercus*, *Castanea* vs *Olea*, *Cedrus*
141 vs *Helianthus*, *Corylus* vs *Quercus*, *Fagus* vs *Helianthus*, *Fagus* vs *Zea*, , and *Phleum* vs *Quercus*, all of which
142 show similar scattering intensities. Although it is not clear if the classification theory introduced above is
143 applicable to these groups, the theory should be applicable to other pairs as long as they have different scattering
144 intensity distributions.

145 The estimation of the pollen counts of *Alnus* and *Artemisia* had average errors of approximately 40% and 23%,
146 respectively. Test 4 had the largest error, with approximately 134% for *Alnus* and approximately 44% for
147 *Artemisia*, which increased the average error. It is difficult to identify an obvious reason for these large values,
148 but it is possible that the pollen samples were contaminated by dusts or pollen grains picked up for this experiment
149 were biased in size or shape.. Additionally, other estimations derived from the fitted curve of the front and the
150 side scattering distributions showed that even when the pollen counts are estimated only from scattering intensity
151 data without using total number of pollen grains, which is a known number, the pollen counts are able to be
152 calculated accurately. The KH-3000-01 has been widely used to estimate airborne concentrations of *Cryptomeria*
153 *japonica*. In this study, we found average errors of 20-40% for *Alnus* and *Artemisia*, values which are also likely
154 applicable to other taxa such as *Cryptomeria japonica*. Other taxa should, however, be investigated in future.

155 Pollen counts can be estimated by solving Eq. (5), which contains three equations, meaning that it is possible to
156 make estimates for three different pollen taxa simultaneously. If more integration intervals were picked up from
157 the probability density curve of the scattering intensity and added to the equation, in theory it would be possible
158 to count more pollen taxa. It is possible, however, that the accuracy of the estimated values might decline due to
159 the accuracy of the fitted curve. Therefore, narrowing down a target to two or three pollen types considering the
160 season should be helpful to make accurate automatic counts of several pollen taxa simultaneously.

161 In this study, the normal distribution function was chosen for fitting because of its universal property. However,
162 further consideration is required to determine the best function for fitting actual light scattering characteristics.

163

164 5 Conclusion

165 By applying the statistical analysis method, the Bonferroni method to the scattering patterns of *Alnus* at each time
166 step, our experiment showed that there seems to be no significant temporal changes in the light scattering patterns.
167 We also confirmed that different pollen types do not always have different light scattering patterns. However,
168 when two different pollen types have different light scattering patterns, it was possible to calculate the number of
169 pollen grains of each taxa using these light scattering patterns by solving the probability density function of the
170 pattern.

171

172 Code/Data availability: The authors confirm that the data supporting the findings of this study are available
173 within the article.

174

175 Author contributions: Kenji Miki established the system, performed the data analysis, and wrote the manuscript.
176 Shigeto Kawashima arranged the experimental setup and proofread the manuscript.

177 Conflict of interest: The authors declare that they have no conflict of interest.

178

179 Acknowledgement

180 This research was supported by the Young Research Exchange Programme between Japan and Switzerland
181 under the Japan-Swiss Science and Technology Programme.

182

183

184



185 **References**

- 186 Boucher, A., Hidalgo, P.J., Thonnat, M., Belmonte, J., Galan, C., Bonton, P., and Tomczak, R.: Development of
187 a semi-automatic system for pollen recognition. *Aerobiologia*, 18, 195–201, 2002.
- 188 Buters, J.T.M., Antunes, C., Galveias, A., Bergmann, K.C., Thibaudon, M., Galán, C., Schmidt-Weber, C., and
189 Oteros, J.: Pollen and spore monitoring in the world. *Clin. Transl. Allergy*, 8, doi.org/10.1186/s13601-
190 018-0197-8, 2018.
- 191 Chen, C., Hendricks, E.A., Duin, R.P.W., Reiber, J.H.C., Hiemstra, P.S., de Weger, L.A., and Stoel, B.C.:
192 Feasibility study on automated recognition of allergenic pollen: grass, birch and mugwort. *Aerobiologia*,
193 22, 275–284. doi:10.1007/s10453-006-9040-0, 2006.
- 194 Crouzy, B., Stella, M., Konzelmann, T., Calpini, B., and Clot, B.: All-optical automatic pollen identification:
195 Towards an operational system. *Atmos. Environ.*, 140, 202–212, 2016.
- 196 France, I. Duller, A.W.G., Duller, G.A.T., and Lamb, H.F.: A new approach to automated pollen analysis. *Quat.*
197 *Sci. Rev.*, 19, 537–546, 2000.
- 198 Gallardo-Caballero, R., García-Orellana, C. J., García-Manso, A., González-Velasco, H., Tormo-Molina, R., and
199 Macías-Macías, M.: Precise pollen grain detection in bright field microscopy using deep learning
200 technique. *Sensors*, 19, 3583. doi:10.3390/s19163583, 2019.
- 201 Gonçalves, A.B., Souza, J.S., de Silva, G.G., Cereda, M.P., Pott, A., Naka, M.H., and Pistori, H.: Feature
202 extraction and machine learning for the classification of Brazilian savannah pollen grains. *PLoS ONE*,
203 11, e0157044. doi:10.1371/journal.pone.0157044, 2016.
- 204 Gottardini, E., Rossi, S., Cristofolini, F., and Benedetti, L.: Use of Fourier transform infrared (FT-IR)
205 spectroscopy as a tool for pollen identification. *Aerobiologia*, 23, 211–219, 2007.
- 206 Huffman, D. R., Swanson, B. E., and Huffman, J. A.: A wavelength-dispersive instrument for characterizing
207 fluorescence and scattering spectra of individual aerosol particle on a substrate. *Atmos. Meas. Tech.*, 9,
208 3987–3998, 2016.
- 209 Iwai, T.: Polarization analysis of light scattered by pollen grains of *Cryptomeria japonica*. *Jpn. J. Appl. Phys.*, 52,
210 062404. doi.org/10.7567/JJAP.52.062404, 2013.
- 211 Kaya, Y., Mesut Pinar, S., Emre Erez, M., Fidan, M., and Riding, J.B.: Identification of *Onopordum* pollen using
212 the extreme learning machine, a type of artificial neural network. *Palynology*, 38, 129–137.
213 doi.org/10.1080/09500340.2013.868173, 2014.
- 214 Kawashima, S., Clot, B., Fujita, T., Takahashi, Y., and Nakamura, K.: An algorithm and a device for counting
215 airborne pollen automatically using laser optics. *Atmos. Environ.*, 41, 7987–7993, 2007.
- 216 Kawashima, S., Thibaudon, M., Matsuda, S., Fujita, T., Lemonis, N., Clot, B., and Oliver, G.: Automated pollen
217 monitoring system using laser optics for observing seasonal changes in the concentration of total airborne
218 pollen. *Aerobiologia*, 33, 351–362, 2017.
- 219 Landsmeer, S.H., Hendricks, E.A., De Weger L.A., Reiber, J.H.C., and Stoel, B.C.: Detection of pollen grains in
220 multifocal optical microscopy images of air samples. *Microsc. Res. Tech.*, 72, 424–430, 2009.
- 221 Li, P., Treloar, W.J., Flenley, J.R., and Empson, L.: Towards automation of palynology 2: the use of texture
222 measures and neural network analysis for automated identification of optical images of pollen grains. *J.*
223 *Quat. Sci.*, 19, 755–762. doi: 10.1002/jqs.874, 2004.
- 224 Longhi, S., Cristofori, A., Gatto, P., Cristofolini, F., and Grando, M.S., Gottardini, E.: Biomolecular identification
225 of allergenic pollen: a new perspective for aerobiological monitoring? *Ann. Allergy Asthma Immunol.*,
226 103, 508–514, 2009.
- 227 Marcos, J.V., Nava, R., Cristóbal, G., Redondo, R., Escalante-Ramírez, B., Bueno, G., Déniz, Ó., González-Porto,
228 A., Pardo, C., Chung, F., and Rodríguez, T.: Automated pollen identification using microscopic imaging
229 and texture analysis. *Micron*, 68, 36–46. doi.org/10.1016/j.micron.2014.09.002, 2015.



- 230 Matsuda, S., and Kawashima, S.: Relationship between laser light scattering and physical properties of airborne
231 pollen. *J. Aerosol Sci.*, 124, 122–132, 2018.
- 232 Miki, K., Kawashima, S., Fujita, T., Nakamura, K., and Clot, B.: Effect of micro-scale wind on the measurement
233 of airborne pollen concentrations using volumetric methods on a building rooftop. *Atmos. Environ.*, 158,
234 1–10. doi.org/10.1016/j.atmosenv.2017.03.015, 2017.
- 235 Miki, K., Kawashima, S., Clot, B., and Nakamura, K.: Comparative efficiency of airborne pollen concentration
236 evaluation in two pollen sampler designs related to impaction and changes in internal wind speed. *Atmos.*
237 *Environ.*, 203, 18–27, doi.org/10.1016/j.atmosenv.2019.01.039, 2019.
- 238 Mitsumoto, K., Yabusaki, K., and Aoyagi, H.: Classification of pollen species using autofluorescence image
239 analysis. *J. Biosci. Bioeng.*, 107, 90–94, 2009.
- 240 Mitsumoto, K., Yabusaki, K., Kobayashi, K., Aoyagi, H.: Development of a novel real-time pollen-sorting counter
241 using species-specific pollen autofluorescence. *Aerobiologia*, 26, 99–111, doi:10.1007/s10453-009-
242 9147-1, 2010.
- 243 O'Connor, D.J., Healy, D.A., and Sodeau, J.R.: The on-line detection of biological particle emissions from selected
244 agricultural materials using the WIBS-4 (Waveband Integrated Bioaerosol Sensor) technique. *Atmos.*
245 *Environ.*, 80, 415–425, doi.org/10.1016/j.atmosenv.2013.07.051, 2013.
- 246 Oteros, J., Pusch, G., Weichenmeier, I., Heimann, U., Möller, R., Röseler, S., Traidl-Hoffmann, C., Schmidt-
247 Weber, C., and Buters, J.T.M.: Automatic and online pollen monitoring. *Int. Arch. Allergy Immunol.*,
248 167, 158–166, doi: 10.1159/000436968, 2015.
- 249 Punyasena, S.W., Tchong, D.K., Wesseln, C., and Mueller, P.G.: Classifying black and white spruce pollen using
250 layered machine learning. *New Phytol.*, 196, 937–944, doi: 10.1111/j.1469-8137.2012.04291.x, 2012.
- 251 Ranzato, M., Taylor, P.E., House, J.M., Flagan, R.C., LeCun, Y., and Perona, P.: Automatic recognition of
252 biological particles in microscopic images. *Pattern Recognit. Lett.*, 28, 31–39,
253 doi:10.1016/j.patrec.2006.06.010, 2007.
- 254 Richardson, S.C., Mytilinaios, M., Foskinis, R., Kyrou, C., Papayannis, A., Pyri, I., Giannoutsou, E., and
255 Adamakis, I.D.S.: Bioaerosol detection over Athens, Greece using the laser induced fluorescence
256 technique. *Sci. Total Environ.*, 696, 133906, doi.org/10.1016/j.scitotenv.2019.133906, 2019.
- 257 Rogríguez-Damián, M., Cernadas, E., Formella, A., Fernández-Delgado, M., and De Sá-Otero, P.: Automatic
258 detection and classification of grains of pollen based on shape and texture. *IEEE Trans. Syst. Man Cybern.*
259 *Syst.*, 36, 531–542, doi:10.1109/TSMCC.2005.855426, 2006.
- 260 Šaulienė, I., Šukienė, L., Daunys, G., Valiulis, G., Vaitkevičius, L., Matavulj, P., Brdar, S., Panic, M., Sikoparija,
261 B., Clot, B., Crouzy, B., and Sofiev, M.: Automatic pollen recognition with the Rapid-E particle counter:
262 the first-level procedure, experience and next steps. *Atmos. Meas. Tech.*, 12, 3435–3452, 2019.
- 263 Surbek, M., Esen, C., Schweiger, G., and Ostendorf, A.: Pollen characterization and identification by elastically
264 scattered light. *J. Biophotonics*, 4, 49–56, doi:10.1002/jbio.200900088, 2011.
- 265 Swanson, B.E., and Huffman, J.A.: Development and characterization of an inexpensive single-particle
266 fluorescence spectrometer for bioaerosol monitoring. *Opt. Express*, 26, 3646–3660, 2018.
- 267 Takahashi, Y., Kawashima, S., Fujita, T., Ito, C., Togashi, R., and Takeda, H.: Comparison between real-time
268 pollen monitor KH-3000 and Burkard sampler. *Arerugi*, 50, 1136–1142, 2011.
- 269 Tchong, D.K., Nayak, A.K., Fowlkes, C.C., and Punyasena, S.W.: Visual recognition software for binary
270 classification and its application to spruce pollen identification. *PLoS ONE*, 11, e0148879,
271 doi:10.1371/journal.pone.0148879, 2016.



- 272 Wang, Q., Nakamura, S., Gong, S., Suzuki, M., Nakajima, D., Takai, Y., Lu, S., Sekiguchi, K., and Miwa, M.:
273 Release behaviour of *Cryptomeria japonica* pollen allergenic cry j1 and cry j2 in rainwater containing
274 air pollutants. *Int. J. Sustain. Dev. Plann.*, 9, 42–53, doi:10.2495/SDP-V9-N1-42-53, 2014.
- 275 Zhang, Y., Fountain, D.W., Hodgson, R.M., Flenley, J.R., and Gunetileke, S.: Towards automation of palynology
276 3: pollen pattern recognition using Gabor transforms and digital moments. *J. Quat. Sci.*, 19, 763–768,
277 doi: 10.1002/jqs.875, 2004.
278



- 279 Figure 1 Light scattering distribution data from *Alnus* and *Artemisia* used for estimation test.
- 280 Figure 2 Light scattering plots for *Alnus* pollen – fresh and after 1h, 2h, 6h, and 10 days storage.
- 281 Figure 3 Light scattering distribution of various pollen taxa.
- 282 Figure 4 Fitted curve for side scattering (top row) and probability density curve (second row) for *Alnus* (left)
- 283 and *Artemisia* (right) and fitted curve for front scattering (third row) and probability density curve (bottom row)
- 284 for *Alnus* (left) and *Artemisia* (right).
- 285 Figure 5 Results of automatic counting of *Alnus* and *Artemisia*. Red and black dots represent actual and
- 286 estimated numbers of pollen grains, respectively. The pair of red and black dots with the same shape are in the
- 287 same test set.
- 288
- 289 Table 1 Multiple comparison between *Alnus* data stored for various periods.
- 290 Table 2 Multiple comparison between each pollen taxon
- 291 Table 3 Results of estimation of number of pollen grains of *Alnus* and *Artemisia* and errors of each estimation.
- 292

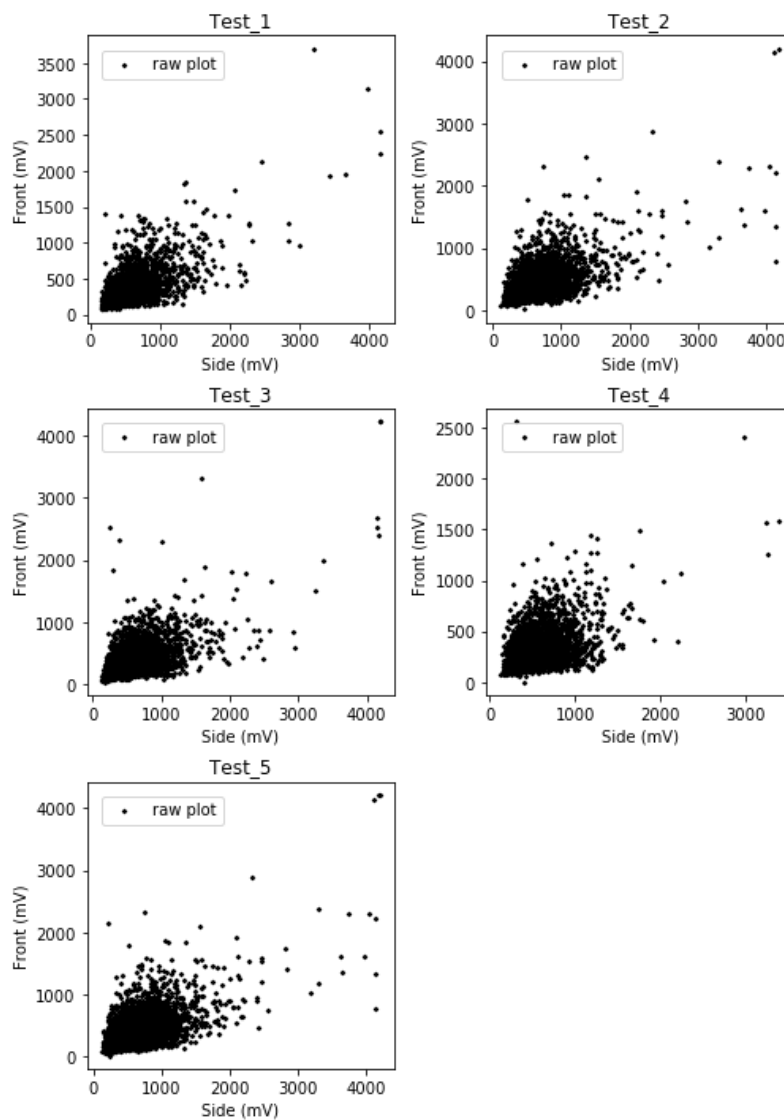


293

294

295

296



297

298 Fig.1

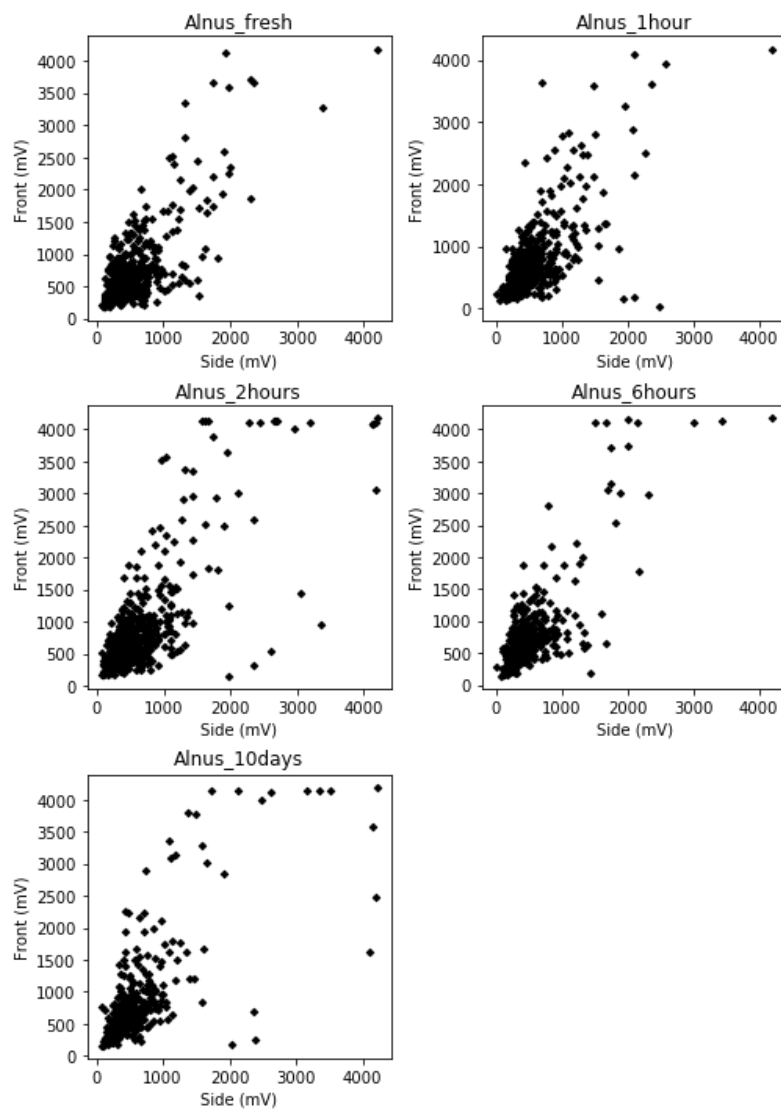
299

300

Miki et al.



301



302

303

304

305

306

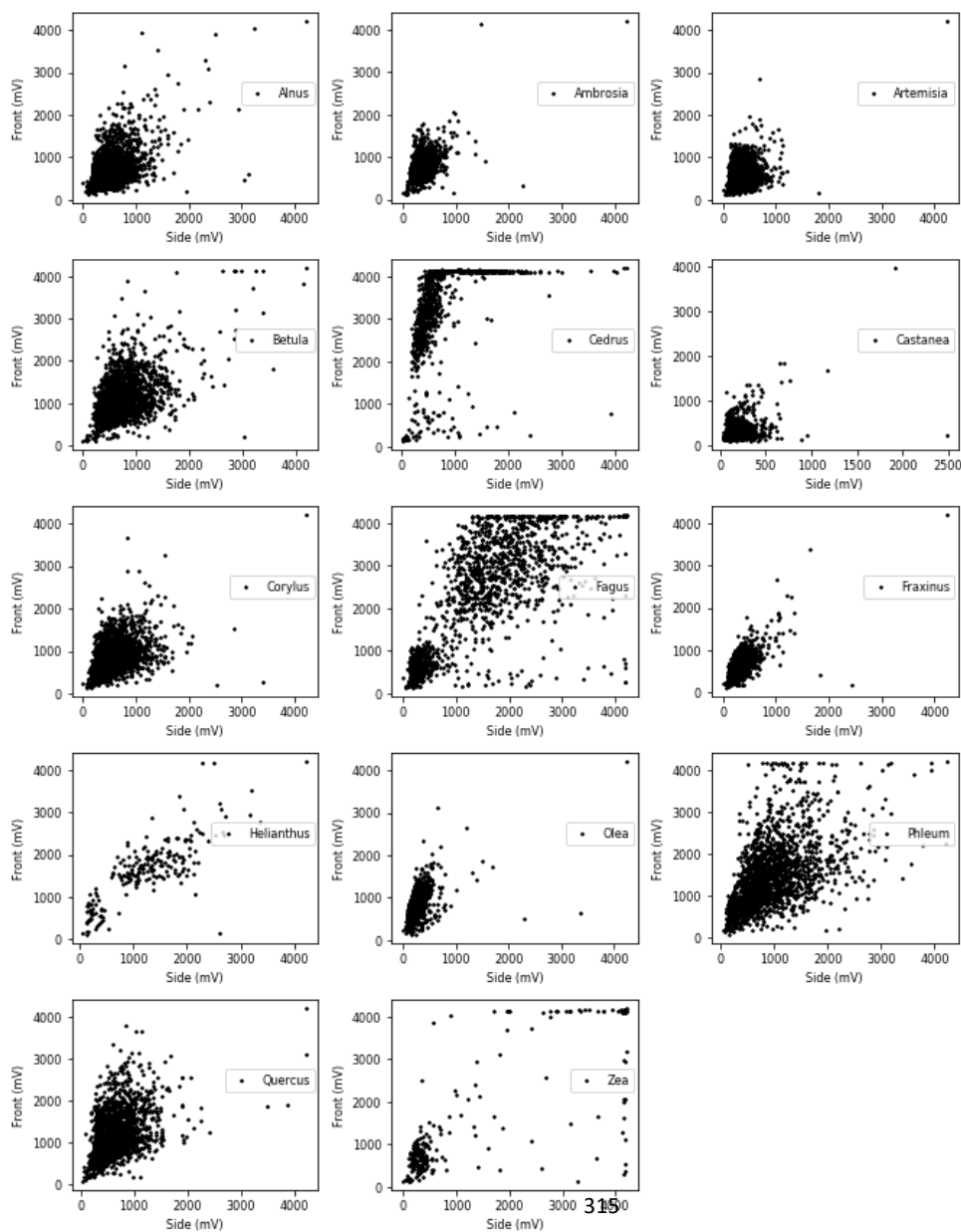
307

308 Fig.2

Miki et al.



309



310

316

317

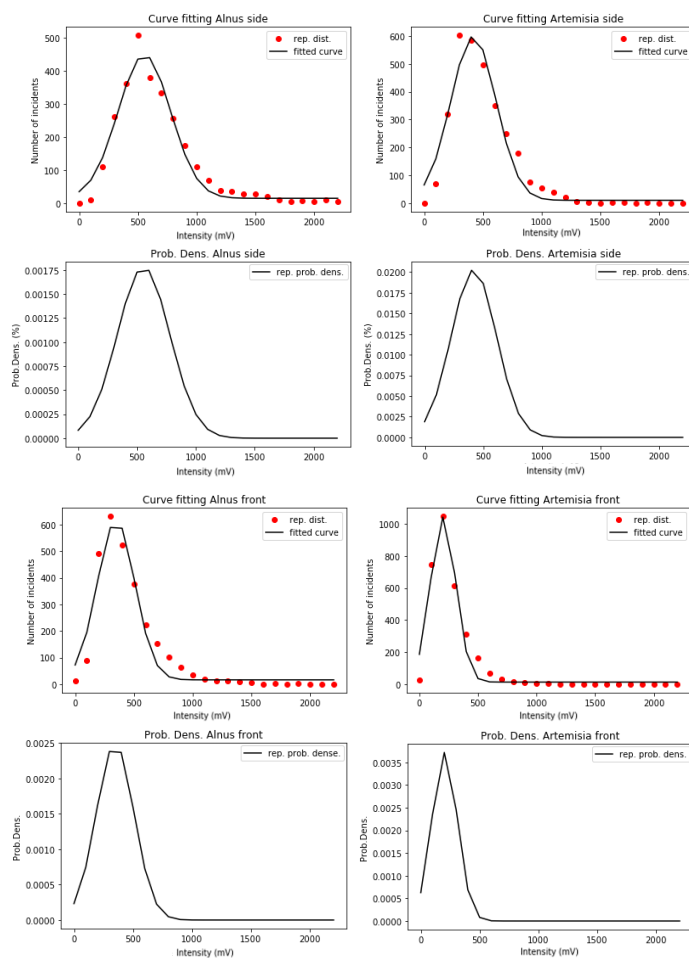
318 Fig.3

319

Miki et al.



320



321

322 Fig.4

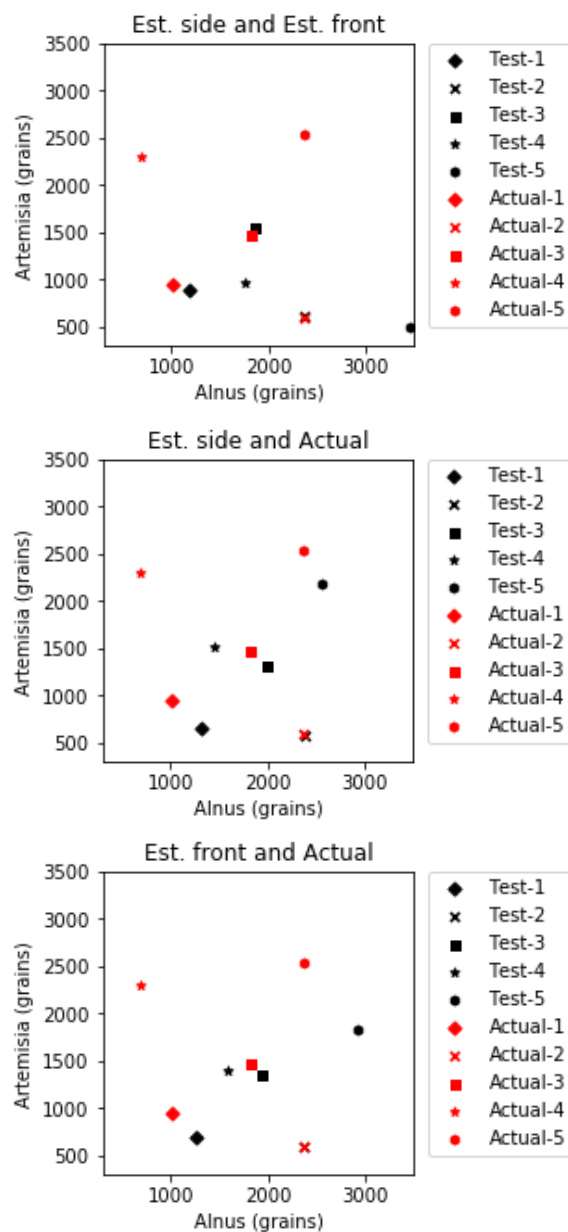
323

324

325

326

Miki et al.



327

328

329 Fig.5

330

331

Miki et al.



332

333

334

335

Table 1 Multiple comparisons between each time step (*Alnus*)

336

Side				
	1hour	2hour	6hour	10day
fresh	1.00	0.38	1.00	1.00
1hour	—	1.00	1.00	1.00
2hour	—	—	0.71	1.00
6hour	—	—	—	1.00

Front				
	1hour	2hour	6hour	10day
fresh	1.00	1.00	1.00	1.00
1hour	—	1.00	0.84	1.00
2hour	—	—	1.00	1.00
6hour	—	—	—	0.31

337

338

339

340

Miki et al.

341

342

343

344



345

346

Table 2 Multiple comparisons between each pollen taxon

Side	<i>Ambrosia</i>	<i>Artemisia</i>	<i>Betula</i>	<i>Castanea</i>	<i>Cedrus</i>	<i>Corylus</i>	<i>Fagus</i>	<i>Fraxinus</i>	<i>Helianthus</i>	<i>Olea</i>	<i>Phleum</i>	<i>Quercus</i>	<i>Zea</i>
<i>Alnus</i>	0.34	*	*	*	*	1.00	*	*	*	1.00	*	*	*
<i>Ambrosia</i>	—	*	*	*	*	*	*	0.08	*	*	*	*	*
<i>Artemisia</i>	—	—	*	*	*	*	*	0.06	*	*	*	*	*
<i>Betula</i>	—	—	—	*	*	*	*	*	*	*	0.06	1.00	*
<i>Castanea</i>	—	—	—	—	*	*	*	*	*	*	*	*	*
<i>Cedrus</i>	—	—	—	—	—	*	*	*	*	*	*	*	*
<i>Corylus</i>	—	—	—	—	—	—	*	*	*	0.49	*	*	*
<i>Fagus</i>	—	—	—	—	—	—	—	*	*	*	*	*	0.59
<i>Fraxinus</i>	—	—	—	—	—	—	—	—	*	*	*	*	*
<i>Helianthus</i>	—	—	—	—	—	—	—	—	—	*	*	*	1.00
<i>Olea</i>	—	—	—	—	—	—	—	—	—	—	*	*	*
<i>Phleum</i>	—	—	—	—	—	—	—	—	—	—	—	1.00	*
<i>Quercus</i>	—	—	—	—	—	—	—	—	—	—	—	—	*

* $p < 0.05$

347

Front	<i>Ambrosia</i>	<i>Artemisia</i>	<i>Betula</i>	<i>Castanea</i>	<i>Cedrus</i>	<i>Corylus</i>	<i>Fagus</i>	<i>Fraxinus</i>	<i>Helianthus</i>	<i>Olea</i>	<i>Phleum</i>	<i>Quercus</i>	<i>Zea</i>
<i>Alnus</i>	*	*	*	*	*	1.00	*	*	*	*	*	1.00	*
<i>Ambrosia</i>	—	0.95	*	*	*	*	*	1.00	*	*	*	*	*
<i>Artemisia</i>	—	—	*	*	*	*	*	1.00	*	*	*	*	*
<i>Betula</i>	—	—	—	*	*	*	*	*	*	1.00	1.00	1.00	*
<i>Castanea</i>	—	—	—	—	*	*	*	*	*	1.00	*	*	*
<i>Cedrus</i>	—	—	—	—	—	*	*	*	1.00	*	*	*	*
<i>Corylus</i>	—	—	—	—	—	—	*	*	*	*	*	1.00	*
<i>Fagus</i>	—	—	—	—	—	—	—	*	0.14	*	*	*	1.00
<i>Fraxinus</i>	—	—	—	—	—	—	—	—	*	*	*	*	*
<i>Helianthus</i>	—	—	—	—	—	—	—	—	—	*	*	*	*
<i>Olea</i>	—	—	—	—	—	—	—	—	—	—	*	*	*
<i>Phleum</i>	—	—	—	—	—	—	—	—	—	—	—	0.10	*
<i>Quercus</i>	—	—	—	—	—	—	—	—	—	—	—	—	*

* $p < 0.05$

349

348

350

351

352

Miki et al.

353

354

355

356



357 Table 3 Results of estimation of number of pollen grains of *Alnus* and *Artemisia* and errors of each estimation.

		Test 1		Test 2		Test 3	
		Alnus (error)	Artemisia (error)	Alnus (error)	Artemisia (error)	Alnus (error)	Artemisia (error)
Estimation	Side and Front	1183 (17.36%)	881 (6.77%)	2367 (0.17%)	612 (3.20%)	1855 (1.76%)	1552 (5.43%)
	Total and Side	1310 (29.96%)	642 (32.06%)	2386 (0.63%)	577 (2.70%)	1984 (8.83%)	1310 (11.01%)
	Total and Front	1259 (24.90%)	694 (26.56%)	2378 (0.30%)	585 (1.35%)	1932(5.98%)	1362 (7.47%)
Actual		1008	945	2371	593	1823	1472

358

		Test 4		Test 5	
		Alnus	Artemisia	Alnus	Artemisia
Estimation	Side and Front	1753 (157.42%)	968 (57.86%)	3469 (57.32%)	489 (80.78%)
	Total and Side	1458 (114.10%)	1520 (33.83%)	2567 (16.42%)	2179 (14.28%)
	Total and Front	1577 (131.57%)	1402 (38.96%)	2929 (32.83%)	1817 (28.92%)
Actual		681	2297	2205	2542

359

362

363

364

365

366

367

Miki et al.